COMMUNICATION

ChemComm
www.rsc.org/chemcomm

Brookite-supported highly stable gold catalytic system for CO oxidation†

Wenfu Yan, Bei Chen, Shannon M. Mahurin, Sheng Dai* and Steven H. Overbury
Chemical Sciences Division, Oak Ridge National Laboratory, Oak Ridge, TN 37831, USA.
E-mail: dais@ornl.gov; Fax: +1 865-576-5235

Received (in Cambridge, UK) 14th April 2004, Accepted 3rd June 2004
First published as an Advance Article on the web 8th July 2004

A significant enhancement of the gold catalysis stability against sintering has been achieved using brookite as a catalytic support.

It has been reported by Haruta and coworkers that the catalytic activity of Au nanoparticles is highly sensitive to the structures of not only gold but also support oxides.[1] Titanium dioxide has been demonstrated to be one of the most effective supports for low-temperature CO oxidation.[2–17] A number of investigations have been devoted to this subject. There are three common crystal phases associated with TiO_2, which are anatase, rutile, and brookite.[18,19] So far, rutile and especially anatase have been extensively investigated as supports for gold nanoparticles in catalytic CO oxidation. The catalytic activities of these two systems are very similar after normalization of support surface areas and gold concentrations. Here, we report a brookite-supported gold catalytic system for CO oxidation. A significant enhancement of the gold catalysis stability against sintering has been achieved using brookite as the support.

Nanosized anatase (≤10 nm) and brookite (~70 nm) particles have been successfully synthesized *via* sonication[20] and hydrothermal methods[21] (see supporting materials for details on syntheses†). Fig. 1 shows the powder XRD patterns of as-synthesized anatase and brookite nanoparticles. The particle sizes were characterized by XRD and SEM micrography. †

Gold precursor was deposited on the surface of the nanosized particles of as-synthesized anatase and brookite supports through a deposition–precipitation (DP) process (see details on DP process†). The XRD patterns of the resulting samples (Fig. 1) show no metallic gold peaks, indicating that no redox reactions happen during the DP process or that the metallic gold particles are not big enough to generate observable XRD peaks.

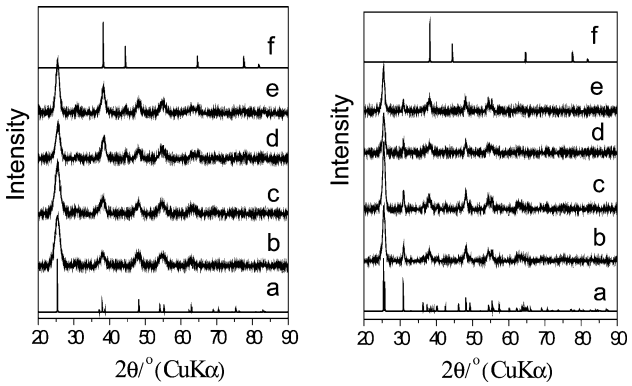

Fig. 1 Left: powder XRD patterns of (a) anatase simulated, (b) anatase as-synthesized, (c) as-synthesized Au–anatase, (d) Au–anatase treated at 300 °C in O_2, (e) Au–anatase treated at 500 °C in O_2, and (f) Au simulated. Right: powder XRD patterns of (a) brookite simulated, (b) brookite as-synthesized, (c) as-synthesized Au–brookite, (d) Au–brookite treated at 300 °C in O_2, (e) Au–brookite treated 500 °C in O_2, and (f) Au simulated.

The CO oxidation reaction was carried out in an AMI 200 (Altamira Instruments). Typically, 50 mg of Au–TiO_2 catalyst was packed into a 4 mm ID quartz U-tube, supported by quartz wool. Sample treatments were carried out on the same instrument using either pre-mixed 8% O_2–He for oxidation or 12% H_2 mixed with He for reduction. During reactions, a gas stream of 1% CO balanced with dry air (< 4 ppm water) was flowed at ambient pressure through the catalyst at a rate that was adjusted from sample to sample to maintain a constant space velocity of 40 000 ml h^{-1} per g of catalyst, or about 37 cm^3 min^{-1}. Gas exiting the reactor was analyzed by a Buck Scientific 910 gas chromatograph equipped with dual molecular sieve/porous polymer column (Alltech CTR1) and a thermal conductivity detector.

The curves (a) and (b) in Fig. 2 compare the light-off curves for the gold catalysts supported on anatase and brookite after being treated with O_2 at 300 °C. Interestingly, the catalytic activity of the brookite-supported gold catalyst remained highly active with the onset for 100% CO conversion around −20 °C. In contrast, the onset for 100% conversion of CO was obtained at 60 °C for the anatase-supported catalyst treated under the same conditions.

The XRD patterns of both catalysts after being treated with O_2 at 300 °C are compared in Fig. 1 (curves (d)). Clearly, the Au–anatase catalyst exhibits gold XRD peaks, indicating the formation of large metallic gold nanoparticles (diameter > 20 Å) on the anatase support. The XRD pattern of the corresponding brookite-supported catalyst gives no XRD peaks associated with the large metallic gold nanoparticles.

The light-off curves of CO oxidation over Au–anatase and Au–brookite catalysts after being treated at 500 °C in O_2 are shown curves (c) and (d), respectively, in Fig. 2. Both catalysts were deactivated by this heat treatment, but the Au–brookite remains significantly more active than the Au–anatase. The onset of 100% CO conversion for the Au–brookite is about 60 °C, while the corresponding onset for the Au–anatase reaches as high as 160 °C. The corresponding XRD patterns of those two samples are shown in Fig. 1 (curves (e)). A very weak gold XRD peak at $2\theta \approx 44.5°$

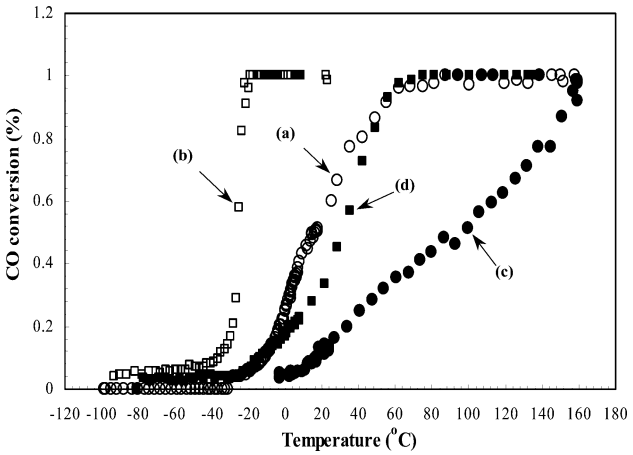

Fig. 2 CO conversion *vs.* reaction temperature over supported Au catalysts: (a) Au–anatase treated at 300 °C in O_2, (b) Au–brookite treated at 300 °C in O_2, (c) Au–anatase treated at 500 °C in O_2, and (d) Au–brookite treated at 500 °C in O_2.

† Electronic supplementary information (ESI) available: details of the syntheses, the deposition–precipitation process and characterization by XRD, BET and SEM. See http://www.rsc.org/suppdata/cc/b4/b405434b/

DOI: 10.1039/b405434b

can be seen in the XRD pattern of Au–brookite treated at 500 °C in O_2, which indicates the formation of a small population of gold nanoparticles > 3 nm *via* sintering. The gold XRD peaks for Au–anatase after being treated with O_2 at 500 °C is more intense than that after being treated with O_2 at 300 °C, which indicates a significant population increase of large gold nanoparticles (> 3 nm). Accordingly, the brookite-supported gold nanoparticles are significantly more stable against the temperature-induced aggregation than the anatase-supported gold nanoparticles.

This assertion about the stability of gold nanoparticles against aggregation on brookite surfaces is also consistent with the microscopy investigation performed using a HD-2000 scanning transmission electron microscope (STEM, probe size 0.3 nm) operating at 200 kV. STEM imaging with a high-angle annular dark-field (HAA-DF) detector provides higher contrast for small clusters of heavy elements in a low atomic number matrix as compared to conventional transmission electron microscopy. The nature of gold nanoparticles deposited on anatase and brookite makes these samples well-suited to HAA-DF (also known as Z-contrast) STEM imaging. Fig. 3 shows the comparison of the dark-field STEM images of the gold catalysts supported on anatase and brookite after being treated with O_2 at 300 °C followed by 500 °C. As seen from Fig. 3, the concentration of the big gold particles (> 3 nm) on brookite is less than that on anatase. However, there is a significant population of small particles (< 2 nm) retained on brookite. Thermally induced growth of particles observed in XRD and STEM was further confirmed by X-ray extended absorption spectroscopy which also clearly indicated that Au supported on anatase sinters more facilely than on brookite.[22] Therefore, the loss of catalytic activity of the gold nanoparticles supported on anatase can be correlated to the higher tendency for the small gold nanoparticles to sinter on anatase during high temperature O_2 treatment.

Further support for the assertion that gold nanoparticles are more susceptible to sintering on anatase than on brookite comes from the analysis of surface areas and gold loadings. The surface area of as-synthesized anatase is 225 $m^2\ g^{-1}$, while it is only 106 $m^2\ g^{-1}$ for the as-synthesized brookite. The gold loadings of Au–anatase and Au–brookite determined *via* an inductively coupled plasma-atomic emission (ICP-AE) are 2.8 wt% and 3.2 wt%, respectively. Thus, gold nanoparticles are more dispersed and should be more stable against sintering on the anatase support if the surface properties of anatase and brookite as well as the interaction between gold nanoparticles and support were similar. This is clearly opposite to the above experimental observation. The difference of the sintering tendency of the gold nanoparticles dispersed on the surface of anatase and brookite must come from the different surface properties of these supports. A stronger interaction between gold nanoparticles and brookite surface or a higher barrier for particle coarsening might exist to slow down the kinetics for movement or thickening of the small gold nanoparticles.[23]

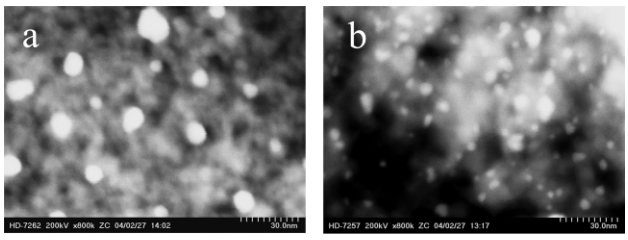

Fig. 3 Dark-field STEM images of the gold catalysts after being treated at 500 °C in O_2: (a) Au–anatase and (b) Au–brookite.

In conclusion, the stability of gold nanoparticles against sintering on brookite and anatase is very different. A highly stable catalytic system for CO oxidation based on the brookite-supported gold catalyst has been developed. The high stability of Au–brookite could result from the unique surface properties of brookite. The interaction between gold nanoparticles and the support plays the important role of stabilizing the catalyst in high temperature environments. Work is underway to explore the applications of the Au–brookite catalyst in other catalytic processes.

This work was conducted at the Oak Ridge National Laboratory and supported by the Office of Basic Energy Sciences, U.S. Department of Energy, under contract No. DE-AC05-00OR22725 with UT-Battelle, LLC. This research was supported in part by an appointment for W.Y., B. C., and S. M. to the Oak Ridge National Laboratory Postdoctoral Research Associates Program administered jointly by the Oak Ridge Institute for Science and Education and Oak Ridge National Laboratory.

Notes and references

1 M. Okumura, S. Tsubota and M. Haruta, *J. Mol. Catal. A.*, 2003, **199**, 73.
2 G. C. Bond and D. Thompson, *Catal. Rev. Sci. Eng.*, 1999, **41**, 319 and references therein.
3 S. Arrii, F. Morfin, A. J. Renouprez and J. L. Rousset, *J. Am. Chem. Soc.*, 2004, **126**, 1199.
4 M. Haruta, S. Tsubota, T. Kobayashi, H. Kageyama, M. J. Genet and B. Delmon, *J. Catal.*, 1993, **144**, 175.
5 M. Valden, X. Lai and D. W. Goodman, *Science*, 1998, **281**, 1647.
6 H. H. Kung, M. C. Kung and C. K. Costello, *J. Catal.*, 2003, **216**, 425.
7 G. J. Hutchings, *Catal. Today*, 2002, **72**, 11.
8 D. C. Meier and D. W. Goodman, *J. Am. Chem. Soc.*, 2004, **126**, 1892.
9 S. D. Lin, M. Bollinger and M. A. Vannice, *Catal. Lett.*, 1993, **17**, 245.
10 M. Okumura, S. Nakamura, S. Tsubota, T. Nakamura, M. Azuma and M. Haruta, *Catal. Lett.*, 1998, **51**, 53.
11 Y. Yuan, A. P. Kozlova, K. Asakura, H. Wan, K. Tsai and Y. Iwasawa, *J. Catal.*, 1997, **170**, 191.
12 G. R. Bamwenda, S. Tsubota, T. Nakamura and M. Haruta, *Catal. Lett.*, 1997, **44**, 83.
13 W. Yan, B. Chen, S. Mahurin, E. W. Hagaman, S. Dai and S. H. Overbury, *J. Phys. Chem. B*, 2004, **108**, 2793.
14 M. A. P. Dekkers, M. J. Lippits and B. E. Nieuwenhuys, *Catal. Lett.*, 1998, **56**, 195.
15 M. Valden, S. Pak, X. Lai and D. W. Goodman, *Catal. Lett.*, 1998, **56**, 7.
16 J. D. Grunwaldt and A. Baiker, *J. Phys. Chem. B*, 1999, **103**, 1002.
17 M. Daté, Y. Ichihashi, T. Yamashita, A. Chiorino, F. Boccuzzi and M. Haruta, *Catal. Today*, 2002, **72**, 89.
18 F. A. Grant, *Rev. Mod. Phys.*, 1959, **31**, 646.
19 G. V. Samsonov, *The Oxide Handbook*, IFI/Plenum Press, New York, 1982.
20 W. Huang, X. Tang, Y. Wang, Y. Koltypin and A. Gedanken, *Chem. Commun.*, 2000, 1415.
21 Y. Zheng, E. Shi, S. Cui, W. Li and X. Hu, *J. Mater. Sci. Lett.*, 2000, **19**, 1445.
22 V. Schwartz, D. R. Mullins, S. Dai and S. H. Overbury, unpublished.
23 C. T. Campbell, *Surf. Sci. Rep.*, 1997, **27**, 1.